

Target State Estimation in an ECM Environment

J.E. Kain* and D.J. Yost†

Applied Physics Laboratory, Silver Spring, Md.

Nonlinear filter techniques of state estimation are applied to a missile intercept problem where the target provides sufficient jamming to deny direct range and range rate measurements. The mathematical model for the measurements and the target dynamics are derived with emphasis on the development of a simplified model for the correlated errors introduced by the inertial reference unit. The nonlinear estimators considered (triangulation, extended Kalman filter, second order Gaussian filter) are evaluated using linearized covariance and Monte Carlo methods. Large initial errors often resulted in poor performance for the extended Kalman filter while the second-order Gaussian filter is found to provide acceptable performance.

Introduction

THE selection of missile guidance policies is in many cases governed by the types of electronic countermeasures (ECM) expected. One form of ECM is the standoff jammer whereby a specially equipped aircraft remains outside the effective missile intercept range and generates electromagnetic interference with sufficient power and appropriate frequency content so that missile fire control radar returns are unintelligible. Since the jammer power required is proportional to range squared while fire control radar power required is proportional to range to the fourth power, the jammer is at an advantage. Thus the intercept missile must be designed to deal with the problems posed by the standoff jammers as well as the higher performance self-screening jammer.

The jamming described above as well as other forms of ECM has the effect of denying target range and range rate information to the intercept missile. Thus, a missile designed to intercept a standoff or self-screening jammer must use a guidance policy that does not require missile to target range or range rate.

Though jamming may prevent target range and range rate measurement, target line of sight (LOS) should be readily available as a missile guidance input. Typically, a modified form of proportional navigation where missile normal accelerations are commanded proportional to missile velocity and missile to target LOS rate is used in an ECM environment. This type of guidance is effective at short ranges, but it does not provide the necessary trajectory shaping for long range intercepts.

In a clear environment where the target position and velocity are available on an uplink from the fire control radar, a midcourse guidance mode is available that shapes the missile trajectory to place the missile close enough to the long range target so that proportional navigation or some other terminal guidance mode may be used. When the missile is restricted to fly proportional navigation over its entire trajectory, the maximum intercept range may be reduced by as much as a factor of two. If no alternate guidance is available, this allows the jammer to stand off at a range considerably less than the maximum clear environment missile intercept range and thus reduces the jamming power required by as much as a factor of four (Fig. 1).

One means of intercepting the long range standoff or self-screening jammer is to use existing midcourse guidance policies but generate estimates of target positions and velocities using only target LOS data. The target LOS should be available from the missile as well as the launch point (designated as a ship). This information, together with the missile position relative to the ship, might be used to solve a triangulation problem and thus to estimate the target location. Target velocity could be estimated by appropriately filtering the position estimate.

Another approach to target estimation is to utilize optimal filtering techniques. The approximate nonlinear optimal filters evaluated here make use of a stochastic model of the target and measurements and offer a considerable improvement in accuracy over the basic triangulation estimate.

In this paper the triangulation estimate, the extended Kalman filter and the second-order Gaussian filter are evaluated as target position and velocity estimators. An attempt was made to consider all potential measurement error sources including the easily modeled uncorrelated errors as well as the highly correlated errors due to the missile inertial system uncertainties. In all cases where specific values are required, data which reflects typical long range intercept missiles are used.

Missile Definition

Before discussing the estimation problem, the nominal missile for which the majority of our studies were performed will be described. The missile will be assumed capable of long-range intercepts on the order of 100 naut miles. A typical long-range trajectory which is the trajectory used for much of

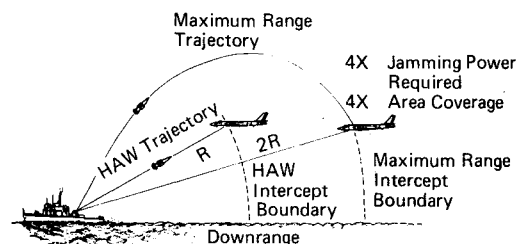


Fig. 1 Extended intercept range for jamming targets.

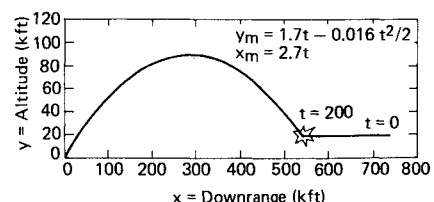


Fig. 2 Missile intercept trajectory for 1000 fps incoming target.

Presented as Paper 74-890 at the AIAA Mechanics and Control of Flight Conference, Anaheim, California, August 5-9, 1974; submitted September 5, 1974; revision received March 6, 1975. This work was supported by Naval Ordnance System Command, Department of the Navy, under Contract N000-17-C-4401.

Index categories: LV/M Guidance Systems (including Command and Information Systems); Tracking Systems.

*Associate Engineer. Member AIAA.

†Senior Engineer.

the analysis is presented in Fig. 2. The missile altitude is given by the following polynomial in time; i.e., $y_m = -0.008t^2 + 1.7t$ (kft). The missile was assumed to maintain a constant downrange velocity of 2.7 kfps. A seeker onboard the missile will be used to track the missile to target LOS in a missile-referenced coordinate system. The pointing errors caused by seeker measurements were assumed zero mean and uncorrelated in time with a data rate of 1 Hz and an rms error of 0.5° .

The missile contains an inertial reference unit (IRU) for determining missile position as well as for determining the inertial missile to target LOS. The error specifications associated with the IRU are given in Table 1.

The ship from which the missile was launched is assumed to track the target LOS to within a zero mean uncorrelated error with an rms of 4 mrad and a data rate of 1 Hz. The nominal data processing rate was chosen as 1 Hz. The data may be processed either onboard the missile (requiring only an uplink) or onboard the ship (requiring both an uplink and downlink). From the standpoint of ECM, an uplink is far more reliable than a downlink and makes the missile processing more attractive.

Measurement Models

The studies performed here will be restricted to the vertical plane analysis, i.e., the ship, missile, and target will be constrained to remain in a vertical plane. The vertical plane target LOS angles from the ship and target (σ_s and σ_m , respectively) are shown in Fig. 3 along with the missile and target Cartesian position (x_m, y_m) and (x_T, y_T), respectively.

The ship to target and missile to target LOS angles σ_s and σ_m are given by

$$\sigma_s = \tan^{-1}(y_T/x_T) \quad (1)$$

and

$$\sigma_m = \tan^{-1} \left[\frac{y_T - y_m}{x_T - x_m} \right] \quad (2)$$

The measured LOS angles σ'_s and σ'_m are modeled by

$$\sigma'_s = \tan^{-1}(y_T/x_T) + \eta_s \quad (3)$$

and

$$\sigma'_m = \tan^{-1} \left[\frac{y_T - y_m}{x_T - x_m} \right] + A_0 + \dot{A}t + \eta_m \quad (4)$$

where t represents the time from missile launch, and η_s and η_m are the uncorrelated measurement errors with nominal statistics: $E(\eta_s) = E(\eta_m) = 0$; $E(\eta_s^2) = (0.004)^2 \text{ rad}^2$; and $E(\eta_m^2) = (0.0057)^2 \text{ rad}^2$. The terms involving A_0 and \dot{A} are the effects of inertial system errors on the measured missile to target LOS angle.

The measured values for missile position (x'_m, y'_m) are modeled as follows:

$$x'_m = x_m + \dot{\epsilon}_x * t - A_0 * y_m \quad (5)$$

$$y'_m = y_m + \dot{\epsilon}_y * t + A_0 * x_m \quad (6)$$

There is assumed to be an independent linear time drift on each axis because of IRU instrument errors plus a term proportional to the initial attitude uncertainty. The initial attitude error tends to rotate the measured position from the actual position so that the position error owing to initial attitude error is orthogonal to the actual position vector (for small rotations). The initial attitude error magnitudes assumed here dominate the position error. For example at the nominal intercept, the one sigma missile altitude error owing to in-

Table 1 Nominal IRU Errors

IRU errors	Symbol	rms error
Gyro drift	\dot{A}	$10^\circ/h$
Initial attitude uncertainty	A_0	0.5°
Instrument dependent	ϵ_x	6 fps
Position drift (per axis)	ϵ_y	

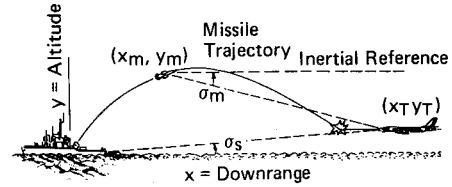


Fig. 3 Vertical plane definitions.

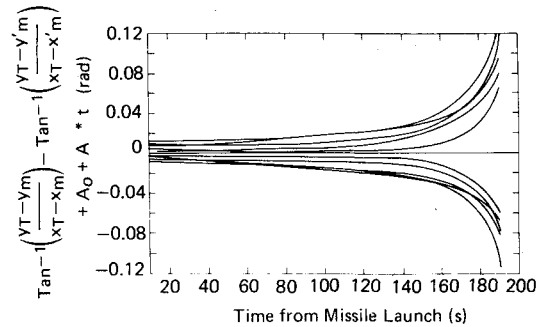


Fig. 4 Inertial system error contribution to missile-to-target LOS.

strument uncertainty is 1.2 kft while the error associated with the initial attitude uncertainty is 4.7 kft.

It should be recognized that the inertial system errors represented in Eqs. (4-6) are approximations of the actual errors. These expressions will nevertheless be used to generate what shall be considered "actual" measurements for the purpose of Monte Carlo studies.

In an attempt to develop an optimal filter for estimating the target states that accounts for the inertial system errors, one approach is to estimate the parameters A_0 , \dot{A} , ϵ_x , and ϵ_y of Eqs. (4-6). This would increase the number of states to be estimated by four and in practice might yield poor or even divergent estimates because of the modeling errors inherent in Eqs. (4-6).

A more realistic measurement model might approximate A_0 , \dot{A} , ϵ_x , and ϵ_y as first-order random processes with large time constants and empirically determined rms levels. This has the effect of "keeping the filter gains open" and masking the effects of system modeling errors. This approach would again increase the filter order by four states.

A model for the measured missile to target LOS which reflects the inertial system errors while adding only a single state is given by

$$\sigma''_m = \tan^{-1} \left[\frac{y_T - y'_m}{x_T - x'_m} \right] + \frac{\beta}{R_{MT}} + \eta_m \quad (7)$$

where

$$\dot{\beta} = \eta_\beta - \beta/\tau_\beta \quad (8)$$

The term R_{MT} is the missile to target range, while the time constant τ_β and the strength of the white noise process η_β define the first order Markov process β . By equating σ''_m to σ'_m , one finds that the stochastic process β/R_{MT} must represent the variable Z are defined by Eq. (9).

$$Z = \tan^{-1} \left[\frac{y_T - y_m}{x_T - x_m} \right] - \tan^{-1} \left[\frac{y_T - y'_m}{x_T - x'_m} \right] + A_0 + \dot{A}t \quad (9)$$

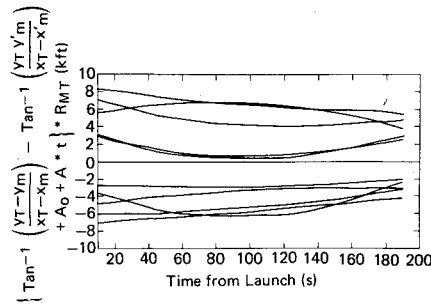


Fig. 5 Inertial system errors multiplied by range.

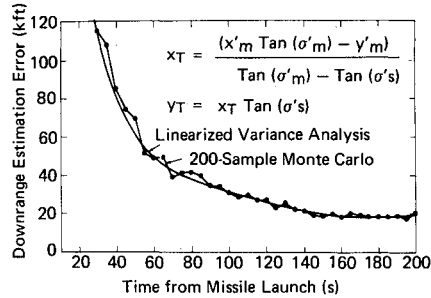


Fig. 6 Standard deviation of downrange estimate using triangulation.

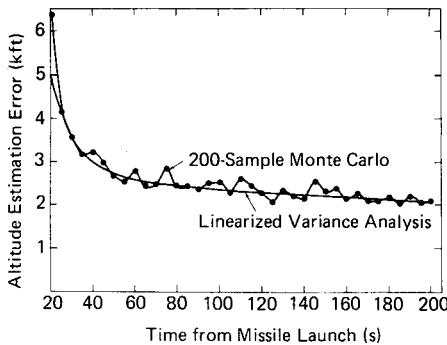


Fig. 7 Standard deviation of altitude estimate using triangulation.

The random time function Z is defined by and summarizes the effect of the inertial system errors on the missile to target LOS. By selecting quantities with the appropriate statistics to represent A_0 , \dot{A} , $\dot{\epsilon}_x$, and $\dot{\epsilon}_y$, the random function Z can be computed over a given missile and target trajectory. Ten such samples of Z are shown in Fig. 4 using the statistics of Table 1 and the trajectory of Fig. 2. If the samples of Fig. 4 are multiplied by R_{MT} , Fig. 5 is the result. The random process $Z \cdot R_{MT}$ was modeled by the first-order Markov process of Eq. (8). The time constant τ_β and the rms of β were selected as 400 sec and 3 kft, respectively.

To develop the optimal filter, Eqs. (3) and (7) will be used to describe the measurements. The use of Eq. (7) to represent the missile to target LOS measurement lies primarily in its simplicity, but, also, the stochastic nature of the process β/R_{MT} should compensate for modeling errors inherent in Eqs. (4-6).

Triangulation Estimate

One estimator for target position is the triangulation estimate. This simple estimator will be evaluated in order to show the improvement realized when optimal filtering theory is applied. In the vertical plane, the triangulation estimate is obtained by solving Eqs. (1) and (2) for x_T and y_T and approximating actual values of σ_m , σ_s , x_m and y_m with measured values. The triangulation estimate (\hat{x}_T, \hat{y}_T) is given by

$$\hat{x}_T = \frac{x'_m \tan(\sigma'_m) - y'_m}{\tan(\sigma'_m) - \tan(\sigma'_s)} \quad (10)$$

$$\hat{y}_T = \hat{x}_T \tan(\sigma'_s) \quad (11)$$

The evaluation of this nonlinear estimator in terms of the statistics of the required measurements can be done approximately using linearized covariance analysis. By defining

$$\hat{Y} = (\hat{x}_T, \hat{y}_T) \quad (12)$$

$$X = (x'_m, y'_m, \sigma'_m, \sigma'_s) \quad (13)$$

Eqs. (10) and (11) can be written vectorially as

$$\hat{Y} = F(X) \quad (14)$$

The covariance of \hat{Y} is approximated by

$$E[(\hat{Y} - Y)(\hat{Y} - Y)^T] = \frac{\partial F}{\partial X} E[(X - \bar{X})(X - \bar{X})^T] \frac{\partial F^T}{\partial X} \quad (15)$$

$$P_{\hat{Y}} = \frac{\partial F}{\partial X} P_X \frac{\partial F^T}{\partial X} \quad (16)$$

where $E[\]$ is the expected value of $\[\]$, \bar{X} is the mean value of X , and $P_{\hat{Y}}$ and P_X are the covariance of \hat{Y} and X , respectively. The partial derivative $\partial F / \partial X$ has elements defined by

$$\left[\frac{\partial F}{\partial X} \right]_{ij} = \frac{\partial F_i}{\partial X_j} \quad (17)$$

The computations implied by Eqs. (16) were performed and the results verified by Monte Carlo simulation. The nominal missile and target were again used. Figures 6 and 7 show typical results.

Figure 6 shows that poor downrange estimation accuracy is to be expected during the early stages of flight prior to about 60 sec. The triangle formed by the ship, missile, and target is very flat in this region making triangulation difficult. During the latter half of flight, downrange estimates are accurate to about 20 kft rms while altitude estimation errors (Fig. 7) are approximately 2 kft rms. Note that, in order to use these estimates to generate acceleration commands, filtering would be required to generate a target velocity estimate as well as smoothed missile acceleration commands.

Note that optimal filtering could be applied at this point by assuming that Eqs. (10) and (11) defined "measurements" with statistics computed according to Eq. (15). This approach requires that all measurements in the vector X be available simultaneously so that the transformation $F(X)$ can be performed—a restriction removed using the more direct filter formulation to be discussed later.

Stochastic Target Model

In order to develop a filter providing more accurate target position estimates as well as velocity estimates, a dynamic target model is required. The estimator should be capable of handling a variety of target trajectories, so a stochastic model is preferred.

The target acceleration along the vertical and horizontal directions are treated as independent first-order Markov processes. This yields the six-state target model of Eqs. (18-23):

$$\dot{A}_x = -A_x / \tau_x + \eta_{A_x} \quad (18)$$

$$\dot{A}_y = -A_y / \tau_y + \eta_{A_y} \quad (19)$$

$$\dot{V}_x = A_x \quad (20)$$

$$\dot{V}_y = A_y \quad (21)$$

$$\dot{x}_T = V_x \quad (22)$$

$$\dot{y}_T = V_y \quad (23)$$

Table 2 Initial target state standard deviations

Target state	Standard deviation at $t=0$
Altitude	10 kft
Range	200 kft
Altitude rate	100 fps
Range rate	1000 fps

The parameters required for defining this target are the statistics of the target states at time zero, the strengths of the white noise processes η_{Ax} and η_{Ay} , and the acceleration time constants τ_x and τ_y . The time constants τ_x and τ_y were selected as 20 sec, and the initial target position and velocity standard deviations are given in Table 2.

Since the target velocity and position states are non-stationary, some analysis is necessary to select appropriate white noise strengths so that target position and velocity states near intercept (taken here as 200 sec) are reasonable. The variances of the target states as functions of time can be computed by solving the differential equation for the propagation of the covariance matrix of the linear system given by Eqs. (18-23).

The approximate target altitude variance ($\sigma_{y_T}^2$) is given by

$$\sigma_{y_T}^2(t) = \sigma_{y_T}^2(0) + \sigma_{v_y}^2(0)t^2 + \sigma_{A_y}^2 \times (2/3 \tau_y t^3 - \tau_y^2 t^2 + 2\tau_y^3) \quad (24)$$

where the strength of the white noise process η_{Ay} is computed to force the y -axis acceleration variance to be constant in time. A similar equation is valid for the downrange target state. The target position and velocity standard deviations at $t=200$ sec for two values of rms target acceleration are given in Table 3.

Table 3 shows that for the initial state variances of Table 2 a target rms acceleration of 21.4 fps² (2/3 g) produces unrealistic target state standard deviations after 200 sec. The value chosen for target rms acceleration for the purpose of filtering was 2.14 fps² or 0.0667 g .

Nonlinear Filtering Problem

The target state estimation problem can now be placed in the format required by the modern optimal estimation techniques. Define the estimator state vector to be

$$X = A_x, A_y, V_x, V_y, x_T, y_T, \beta \quad (25)$$

The state dynamics in continuous form are given by

$$\dot{X} = \begin{bmatrix} -1/\tau_v & 0 & 0 & 0 & 0 & 0 & 0 \\ 0 & -1/\tau_\xi & 0 & 0 & 0 & 0 & 0 \\ 1 & 0 & 0 & 0 & 0 & 0 & 0 \\ 0 & 1 & 0 & 0 & 0 & 0 & 0 \\ 0 & 0 & 1 & 0 & 0 & 0 & 0 \\ 0 & 0 & 0 & 1 & 0 & 0 & 0 \\ 0 & 0 & 0 & 0 & 0 & 0 & -1/\tau_\beta \end{bmatrix} X + \begin{bmatrix} \eta_{Ax} \\ \eta_{Ay} \\ 0 \\ 0 \\ 0 \\ 0 \\ \eta_\beta \end{bmatrix} \quad (26)$$

Table 3 Target state standard deviations near intercept

Target state	Target rms	acceleration
	2.14 fps ²	21.4 fps ²
Altitude	23.5 kft	75.6 kft
Range	283 kft	292 kft
Altitude rate	224 fps	2000 fps
Range rate	1020 fps	2240 fps

The measurement vector available at times t_i designated as Y is given by

$$\begin{bmatrix} \tan^{-1} \frac{(X_6 - y'_m)}{(X_5 - x'_m)} + \frac{X_7}{R_{MT}} + \eta_{mi} \\ Y_i = \tan^{-1} \left[\frac{X_6}{X_5} \right] + \eta_{si} \end{bmatrix} \quad (27)$$

where (x'_m, y'_m) is the measured missile position and η_{mi}, η_{si} are independent zero mean Gaussian sequences.

Though optimal filters for continuous systems with discrete measurements are available in the literature the approach used here will be to first discretize the continuous dynamics and use the fully discrete optimal filters. The discretization of the system of Eq. (26) is given by Eq. (28)

$$X_{i+1} = \Phi X_i + \eta_i \quad (28)$$

$$\Phi = \begin{bmatrix} e^{-T/\tau_x} & 0 & 0 & 0 & 0 & 0 & 0 \\ 0 & e^{-T/\tau_y} & 0 & 0 & 0 & 0 & 0 \\ T & 0 & 1 & 0 & 0 & 0 & 0 \\ 0 & T & 0 & 1 & 0 & 0 & 0 \\ T^2/2 & 0 & T & 0 & 1 & 0 & 0 \\ 0 & T^2/2 & 0 & T & 0 & 1 & 0 \\ 0 & 0 & 0 & 0 & 0 & 0 & e^{-T/\tau_\beta} \end{bmatrix}$$

$$\eta_i = \begin{bmatrix} \omega_x \\ \omega_y \\ 0 \\ 0 \\ 0 \\ 0 \\ \omega_\beta \end{bmatrix}$$

where T is the sample period or the measurement data interval.

The statistics of the zero mean uncorrelated sequences $\omega_{xi}, \omega_{yi}, \omega_{\beta i}$ are given by

$$E(\omega_{xi}^2) = (1 - e^{-2T/\tau_x}) (0.00214 \text{ fps}^2)^2$$

$$E(\omega_{yi}^2) = (1 - e^{-2T/\tau_y}) (0.00214 \text{ fps}^2)^2$$

$$E(\omega_{\beta i}^2) = (1 - e^{-2T/\tau_\beta}) (3 \text{ kft})^2$$

The estimation problem described by Eqs. (27) and (28) has discrete linear state dynamics and discrete nonlinear measurements. This problem falls into the class of nonlinear filtering problems frequently approached using the extended

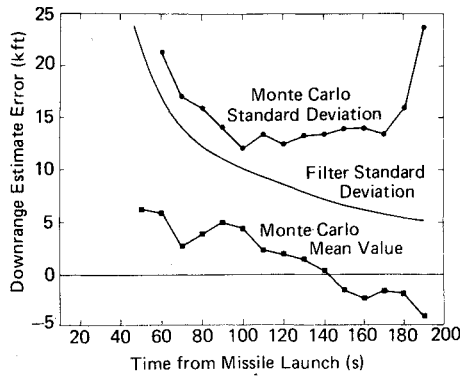


Fig. 8 Downrange estimate for extended Kalman filter.

Kalman filter. When the extended Kalman filter fails to provide satisfactory results the second-order Gaussian filter¹ is available. Since the estimation problem described above has linear dynamics, only the "measurement processing" portion of the second-order Gaussian filter is required.

The computations necessary for the extended Kalman filter and the second-order filter are given below.

$$\tilde{X}_{i+1} = \Phi_i \tilde{X}_i \quad (29)$$

$$P_{i+1}^- = \Phi_i P_i^+ \Phi_i^T + Q \quad (30)$$

$$K_{i+1} = P_{i+1}^- \frac{\partial H^T}{\partial X} \left[\frac{\partial H}{\partial X} P_{i+1}^- \frac{\partial H^T}{\partial X} + R + L \right]^{-1} \quad (31)$$

$$\hat{X}_{i+1} = \tilde{X}_{i+1} + K_{i+1} [(Y - H(\tilde{X}_{i+1}) + \mu)] \quad (32)$$

$$P_{i+1}^+ = \left[I - K_{i+1} \frac{\partial H}{\partial X} \right] P_{i+1}^- \quad (33)$$

The following linear dynamics are assumed:

$$X_{i+1} = \Phi_i X_i + \eta_i; \quad E[\eta_i \eta_j^T] = Q \delta_{ij} \quad (34)$$

where δ_{ij} is the Kronecker delta function, and the discrete nonlinear measurement

$$Y_i = H(X_i) + \omega_i; \quad E[\omega_i] = 0; \quad E[\omega_i \omega_j^T] = R$$

where ω_i is a vector of independent zero mean Gaussian sequences.

The computations for the extended Kalman filter consist of Eqs. (29-33) with $L_{ij} = 0$; $\mu_i = 0$; for all i and j . For the second-order Gaussian filter

$$\mu_i = \frac{1}{2} \sum_{j=1, k=1}^n \frac{\partial^2 H_i}{\partial X_j \partial X_k} P_{jk}^- \quad (35)$$

$$L_{ij} = \frac{1}{2} \sum_{p,q,r,s} \frac{\partial^2 H_i}{\partial X_p \partial X_q} \frac{\partial^2 H_j}{\partial X_r \partial X_s} P_{pr}^- P_{qs}^- \quad (36)$$

At first glance, Eqs. (35) and (36) appear quite formidable. In particular, the computations required for L_{ij} increase as n^4 for an n th order state vector. This is significant when one considers that in general the computation of the extended Kalman filter is proportional to n^3 and lower powers of n .² Thus for large n the L_{ij} computation may dominate the filter computational requirements.

When the measurement equation is a function of only two states (say r and s) the computation can be reduced significantly. Equations (35) and (36) can be reduced to

$$\begin{aligned} \mu_i = \frac{1}{2} \left[\frac{\partial^2 H_i}{\partial X_r \partial X_r} P_{rr}^- + 2 \frac{\partial^2 H_i}{\partial X_r \partial X_s} P_{rs}^- \right. \\ \left. + \frac{\partial^2 H_i}{\partial X_s \partial X_s} P_{ss}^- \right] \quad (37) \end{aligned}$$

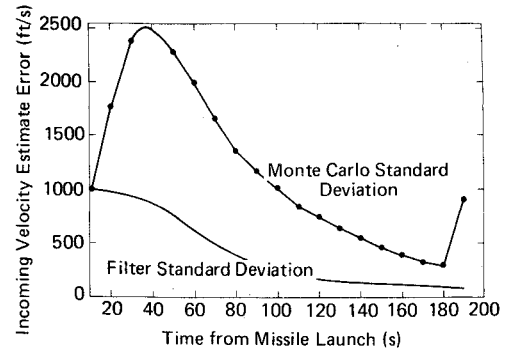


Fig. 9 Incoming velocity estimate for extended Kalman filter.

$$\begin{aligned} L_{ij} = \frac{1}{2} \left[P_{rr}^- P_{ss}^- - P_{rs}^2 \right] \left[2 \frac{\partial^2 H_i}{\partial X_r \partial X_s} \frac{\partial^2 H_j}{\partial X_r \partial X_s} \right. \\ \left. - \frac{\partial^2 H_i}{\partial X_r \partial X_r} \frac{\partial^2 H_j}{\partial X_s \partial X_s} \right. \\ \left. - \frac{\partial^2 H_i}{\partial X_s \partial X_s} \frac{\partial^2 H_j}{\partial X_r \partial X_r} \right] + 2\mu_i \mu_j \quad (38) \end{aligned}$$

These additional computations are insignificant when compared to the seven-state extended Kalman filter computations.

An additional simplification as suggested by Choe³ which will be investigated is an approximation of Eq. (36) by $L_{ij} = 2\mu_i \mu_j$. To evaluate the performance of these filter, the statistics of the estimate errors are required. If the measurement equation were linear, the covariance after measurement (P^+) from Eq. (33) would be used. The square root of the diagonal elements of this matrix yields the standard deviation of the state estimate errors. The filters described above are derived from expansions of the nonlinear measurement equation about the estimate of the state prior to measurement (\tilde{X}_{i+1}). Therefore the covariance matrix after measurement as computed by Eq. (33) is only an approximation.

Thus, to evaluate the nonlinear filters, an additional computation must be made of the state estimation error statistics. This is accomplished via Monte Carlo methods whereby statistically accurate measurements are processed to generate realizations of the target state estimates and the associated errors over a typical missile and target trajectory. From a number of such error histories the ensemble statistics (mean and standard deviations) are computed. These statistics may be compared with those predicted by the nonlinear filter. Good correlation between the Monte Carlo and filter predicted standard derivations is an indication that the nonlinear functions involved are sufficiently smooth in the region about the actual states so that the nonlinear filter yields a "near" optimal estimate.

Nonlinear Filtering Results

For the Monte Carlo studies discussed here, the actual target and missile trajectories were fixed while generating each of the state error histories. The initial state estimates and the measurement error sequences are selected based on their prescribed statistics.

The Monte Carlo study with fixed-target trajectory was performed using an intercept scenario similar to that shown by Fig. 2; i.e., the target is incoming at 20 kft altitude and 1000 fps velocity and is intercepted at 200 sec from missile launch. Simulated measurements based on statistical realizations of Eqs. (3-6) were computed over the missile flight at a 1 Hz data rate. Twenty-five measurement histories were generated together with the corresponding target state estimates for the purpose of computing the Monte Carlo statistics. For initialization of the filter, it was assumed that prior to missile launch an estimate of the target states was available with

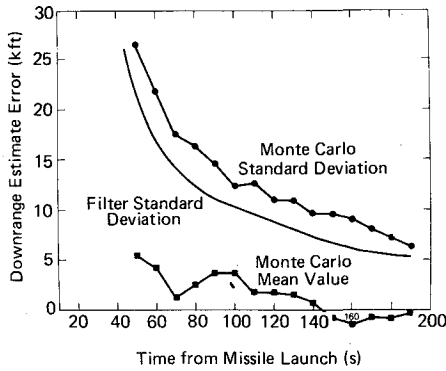


Fig. 10 Downrange estimate for extended Kalman filter with nonlinear bias compensation.

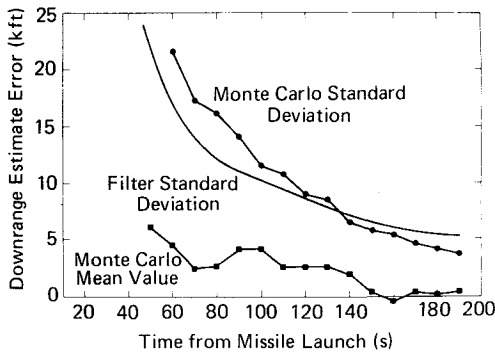


Fig. 11 Downrange estimate for second-order Gaussian filter.

mean value equal to the actual value and standard deviations as given by Table 2.

Some results from the Monte Carlo analysis for the extended Kalman filter are seen in Figs. 8 and 9. Note that the downrange target position (Fig. 8) and velocity (Fig. 9) Monte Carlo statistics differ markedly from the extended Kalman filter prediction.

From an inspection of the individual trajectories it was discovered that by "removing" several of the "poor" estimate histories from the Monte Carlo computation, good agreement between the predicted and computed statistics could be obtained. Also in most cases the poor target estimate histories coincided with large initial target position errors. This is an indication that the region of measurement equation linearity is not sufficiently large to include the region of probable target state estimates early in missile flight. This problem can be overcome to some extent by providing more accurate initial target estimates.

In order to improve the region of acceptable filter performance the second-order Gaussian filter was applied. Based on the experimental results with the particular nonlinear estimation problem investigated in Ref. 1 it would appear that the major improvement in using the second-order Gaussian filter would come from only the bias compensation term (μ). In Ref. 2, the opposite effect is noticed; i.e., the improvement is attributed solely to the gain compensation term (L). When the second-order Gaussian filter is applied to the problem presented here, both nonlinear terms affect the estimation accuracy. When only the bias compensation term (μ) is added to the filter equations and the identical measurement sequences used in generating Figs. 8 and 9 are processed, the divergent cases noted with the extended Kalman filter did not appear. The downrange filter performance with only the bias compensation term is shown in Fig. 10. Note that the Monte Carlo standard deviation is higher than the predicted standard deviation. When the complete second-order Gaussian filter was implemented the correlation of Figs. 11-14 was observed. These four figures show the Monte Carlo standard deviations in good agreement with (or below) the filter predic-

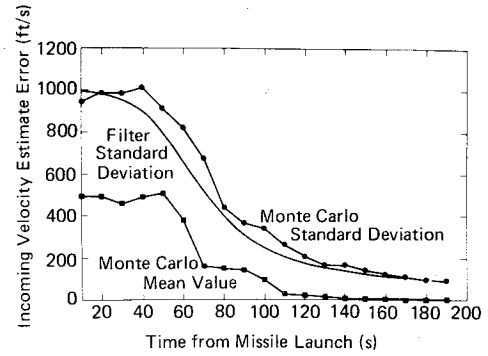


Fig. 12 Incoming velocity estimate for second-order Gaussian filter.

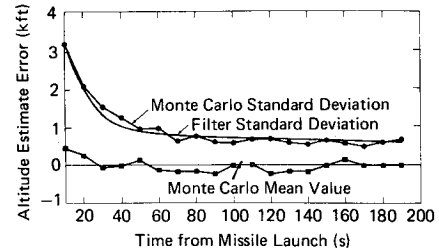


Fig. 13 Altitude estimate for second-order Gaussian filter.

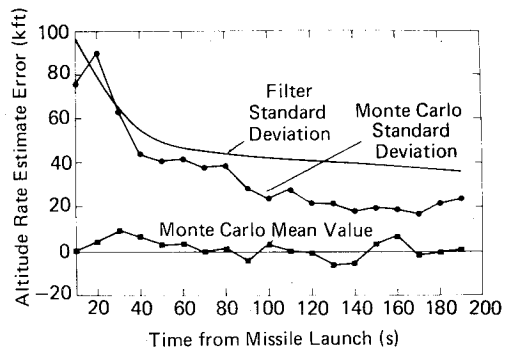


Fig. 14 Altitude rate estimate for second-order Gaussian filter.

tions for both downrange and vertical positions and velocities.

It should be noted that the filter used by Choe in Ref. 3 was somewhat different from the filter derived by Athans in Ref. 1. Choe approximates the gain compensation term (L) by

$$L_{ij} \approx 2\mu_i \mu_j \quad (39)$$

rather than using Eq. (36). When the approximation of Eq. (39) is used with the estimator discussed here, the results are identical to Figs. 11-14. It should also be noted that the estimator performance as indicated by Figs. 11-14 not only represents an evaluation of the particular filtering algorithms but also verifies the use of Eq. (7) as an approximation to the measurement model.

As with the triangulation estimate the target estimation accuracy is poor early in flight but improves as intercept approaches to a more or less steady-state value. Note that the optimal filtering technique has improved the position estimation by a factor of more than three as well as having provided a filtered velocity estimate.

Conclusions

This paper has presented a possible solution to a problem of ever increasing importance in the light of advances in modern warfare—namely missile long range guidance without target range data. The target state estimation accuracy achieved

using the second-order Gaussian filter to process the available target line-of-sight measurements should be sufficient to allow handover to terminal guidance.

The advantages of modern filtering techniques are demonstrated by the significant improvement in estimation accuracy as compared with a more classical estimation approach. It is shown that for the nonlinear multiple-measurement filtering problem, presented here, the complete second-order Gaussian filter provides improved performance over the extended Kalman filter as well as the extended Kalman filter with a nonlinear bias correction term.

References

- ¹Athans, M., Wishner, R.P., and Bertolini, A., "Suboptimal State Estimation for Continuous Time Nonlinear Systems from Discrete Noisy Measurements," *1968 Joint Automatic Control Conference*, Ann Arbor, Mich., June 1968, pp. 364-382.
- ²Mendel, J.M., "Computational Requirements for a Discrete Kalman Filter," *IEEE Transactions on Automatic Control*, Vol. AC-16, No. 6, Dec. 1971, pp. 748-758.
- ³Tapley, B.D. and Choe, C.Y., "Nonlinear Estimation Theory Applied to The Interplanetary Orbit Determination Problem," *Third Symposium on Nonlinear Estimation Theory and its Applications*, Sept. 1972, pp. 239-245.

From the AIAA Progress in Astronautics and Aeronautics Series . . .

THERMOPHYSICS—APPLICATIONS TO THERMAL DESIGN OF SPACECRAFT—v. 23

Edited by Jerry T. Bevans, TRW Systems

The thirty-six papers in this volume are concerned with experimental thermophysical properties, prediction of such properties, and thermal design of spacecraft systems.

Experimental studies report on loading of insulation, contact conductance, gas conductivity, and various properties of cryogenic insulations. Reflectance of various surfaces and methods of measurement, and aging characteristics of various mirror materials, are studied. Phase change processes in spacecraft thermal control are explored.

Analytical predictions are concerned with an albedo model, Monte Carlo prediction of normal and directional emittance, thermal radiation from rough surfaces, and thin film effects on metal surface radiation.

Spacecraft systems thermal design concerns space radiators, heat pipes, thermal control weight and power requirements for life support systems, a thermal system for a landed spacecraft on Mars, considering the widest possible variety of missions and situation for thermal load. Other studies examine requirements for an unmanned lunar lander in all phases of operation, and the roles of mathematical models in augmenting and verifying thermal design practices.

578 pp., 6 x 9, illus. \$21.00 Mem. & List

TO ORDER WRITE: Publications Dept., AIAA, 1290 Avenue of the Americas, New York, N. Y. 10019